IEEE Access
Multidisciplinary | Rapid Review | Open Access Journal

Received 19 September 2022, accepted 6 October 2022, date of publication 13 October 2022, date of current version 19 October 2022.

Digital Object Identifier 10.1109/ACCESS.2022.3214315

RESEARCH ARTICLE

Load Frequency Control of Distributed Generators Assisted Hybrid Power System Using QOHSA Tuned Model Predictive Control

AKSHAY KUMAR[1], NEETU KUMARI[2], GAURI SHANKAR[2], (Member, IEEE), RAJVIKRAM MADURAI ELAVARASAN[3], SACHIN KUMAR[4], (Senior Member, IEEE), ANKIT KUMAR SRIVASTAVA[5], AND BASEEM KHAN[6], (Senior Member, IEEE)

[1]Department of Electrical Engineering, National Sun Yat-sen University, Kaohsiung City 804, Taiwan
[2]Department of Electrical Engineering, Indian Institute of Technology (Indian School of Mines) Dhanbad, Dhanbad, Jharkhand 826004, India
[3]School of Information Technology and Electrical Engineering, The University of Queensland, St. Lucia, QLD 4072, Australia
[4]Department of Electrical Engineering, Govind Ballabh Pant Institute of Engineering and Technology, Pauri-Garhwal, Uttarakhand 246194, India
[5]Department of Electrical Engineering, Institute of Engineering and Technology, Dr. Rammanohar Lohia Avadh University, Faizabad, Uttar Pradesh 224001, India
[6]Department of Electrical and Computer Engineering, Hawassa University, Awassa 1530, Ethiopia

Corresponding authors: Gauri Shankar (gaurishankar@iitism.ac.in) and Baseem Khan (baseem.khan04@gmail.com)

ABSTRACT One of the challenging issues in a hybrid power system (HPS) is to provide a stable power supply with minimum frequency deviation, which can be accomplished by ensuring a coordinated operation among intermittent type distributed generators (DGs). In this study, the coordinated operation of a tidal turbine generator (TTG) (an emerging and less explored DG), diesel engine generator (DEG) and plug-in hybrid electric vehicles (PHEVs) based an autonomous HPS (a less explored HPS of this kind) for load frequency control (LFC) is investigated. The coordinated operation of different control loops such as the blade pitch control loop of TTG, supplementary control loop of DEG, and power control loop of PHEVs are realized through the maiden application of the proposed quasi-oppositional harmony search algorithm (QOHSA) based model predictive control (MPC) strategy. To establish the superiority of the proposed QOHSA tuned MPC method in mitigating frequency deviation following disturbance, its performance is compared with that of the coordinated performance obtained using QOHSA tuned conventional controllers and other existing optimization algorithms. The results conclude that the suggested method can significantly reduce frequency fluctuation under different load disturbances. The proposed method can handle different variances of the disturbance signals or noise entering the system as well as the model mismatch.

INDEX TERMS Hybrid power system, load frequency control, model predictive control, quasi-oppositional harmony search algorithm, tidal turbine generator.

I. INTRODUCTION

In a hybrid power system (HPS), load demand, as well as the power generated from distributed generators (DGs), are dynamic, and thus, the control of DGs is required for reliability enhancement and to reduce the operational cost of the power system [1]. A HPS either operates in an isolated or interconnected mode with the power grid. The benefits of DGs (which is a small and modular type power generation systems located near the consumer site) include reduction of standby generating units in the system, improved flexibility in locating new power plants, and high-quality service to the consumers. The penetration of renewable source-based DGs into existing power systems has been increasing, especially, because of the ample availability of renewable energy sources and their low impact on the environment. However, the presence of uncontrolled/intermittent type DGs such as wind turbine generator (WTG) or tidal turbine generator (TTG) in an HPS may cause a significant frequency fluctuation issues [2], [3]. In addition, system parameters such as inertia constant and damping ratio are also affected, which further deteriorates the overall system stability [4]. To resolve

The associate editor coordinating the review of this manuscript and approving it for publication was Guillermo Valencia-Palomo.

This work is licensed under a Creative Commons Attribution 4.0 License. For more information, see https://creativecommons.org/licenses/by/4.0/

the frequency and stability issues, efficient control strategies need to be formulated for HPS model [5], [6].

Intermittent units like WTGs and TTGs usually operate at the maximum power point (MPP), hence, they cannot contribute to alleviating generation-load imbalance. Thus, intermittent units are exclusive to the load frequency control (LFC) services provided by the utilities following any system events. As per the recent grid code requirements, participation of these units in the frequency regulation process has now become imperative and inevitable to ensure stability. This mandates the formulation of distinct control strategies for intermittent units and in this regard, some attempts have been made by researchers around the globe. In [7], particle swarm optimization (PSO) algorithm-based tuned blade pitch angle control has been implemented on deloaded WTG (which refers to shifting of the operating point of WTG from MPP to a reduced power level) to control power output at steady-state. Authors in [8] have investigated generalized predictive control oriented blade pitch angle control of WTG to achieve stable operation under a rapid change in wind speed. However, regulating the blade pitch angle alone is not always sufficient to deliver constant power output to the consumers. Moreover, frequent adjustment of the blade pitch angle of WTG through the pitch angle control may increase wear and tear [9]. As a solution to the above conundrum, researchers emphasized a hybrid combination of WTG and conventional power generator such as diesel engine generator (DEG) to supply steady power output to the consumers. Coordinated control of WTG and DEG may efficiently reduce frequency deviation and bolster WTG to create a power reserve margin to respond to any load disturbance [9]. Vidyanandan and Senroy [10] have examined the response of WTG in the presence of DEG to curb the frequency deviation in an HPS. In [11], a quasi-oppositional harmony search algorithm (QOHSA) based the optimal LFC of an isolated HPS comprising WTG and DEG is discussed.

Compared to WTG and DEG in HPS, plug-in hybrid electric vehicles (PHEVs) provide a swift response to minimize the frequency deviation following any disturbance in the system. The high-performance attributes and bi-directional charging and discharging capability make it popular in HPS to curb undesirable frequency deviation [12], [13]. PHEVs may be used on the consumer side due to low-cost charging and contribution to reducing greenhouse gas emissions. In the past, to get an optimum frequency regulation, studies on the effect of the presence of PHEVs equipped with various control topologies realized using robust proportional-integral (PI)s controller have been carried out [4]. Further, research concludes that the coordinated control of PHEVs with other generating units may efficiently improve the frequency regulation task. In [4], the coordinated control of PHEVs, DGs and conventional power generator is used to check frequency deviation in the HPS.

TTG is emerging as a new form of DG and has a huge potential like WTG in bridging the gap between electrical energy demand and generation without harming the environment. The operation of TTG is similar to that of WTG [14]. However, its operational aspect and participation in various ancillary services provided by the utilities need to be further explored. Particularly, the literature survey reveals that only meager studies focus on the LFC performance of TTG-assisted HPS. The impact of TTG on power system operation is discussed [15]. Authors in [14] investigated the dynamic behavior of a pitch-regulated TTG. QOHSA-based LFC of HPS (in which the power output of deloaded TTG is controlled by blade pitch angle) is presented [16]. In [16], the authors have also showcased that the QOHSA tuned conventional controllers yields encouraging results in comparison to other algorithms such as PSO, genetic algorithm (GA) and teaching learning-based optimization (TLBO) technique. In most cases, LFC is achieved based on conventional controllers (like PI, proportional integral derivative (PID) controller, etc.) and tuning of these controller's parameters is carried out using a heuristic approach [17]. Even in the presence of a tuned PID controller, degraded performance of LFC may be observed due to the poor handling of system constraints and uncertainties introduced by these controllers [18]. To overcome the aforementioned challenges of conventional controllers, researchers are attracted towards non-traditional types of control methods such as model predictive control (MPC) due to its fast response, robustness, stability against parameter variations, and ease of handling uncertainties and constraints. The main advantages of MPC over conventional controllers are its ability to handle multi-variable systems accurately and to yield controlled frequency variation [19]. In [20], the fundamentals of the MPC method are detailed. In [21], blade pitch angle control of WTG using MPC for LFC is discussed. To enhance the damping of systems, optimal design of LFC using bat optimization algorithm tuned MPC is studied [22].

The literature survey reveals that the performance analysis of LFC of different TTG-assisted HPS models (comprising other types of DGs and conventional units) is less explored, which is one of the scopes of the present study. Owing to the limitations of conventional controllers, MPC is used for stabilizing frequency following a perturbation in the studied system. Nevertheless, proper tuning of MPC is of the utmost to exploit its potential. Therefore, a powerful, simple, and competitive QOHSA (a less explored algorithm in terms of solving power systems' issues) is employed to tune MPC. It has been observed from the past studies, many researchers attempted to give the improved version of the various existing algorithms employing opposition-based learning in population initialization [23], [24], [25], which has offered better results than their basic version. Further to the above, quasi-opposition-based learning has offered even further improved results over the opposition-based learning [26]. Thus, QOHSA is an improved version to both opposition-based learning and its first version [27]. It avoids trapping into local minima and offers quick convergence to near-optimal solutions [23]. The contributions of the present work are given below:

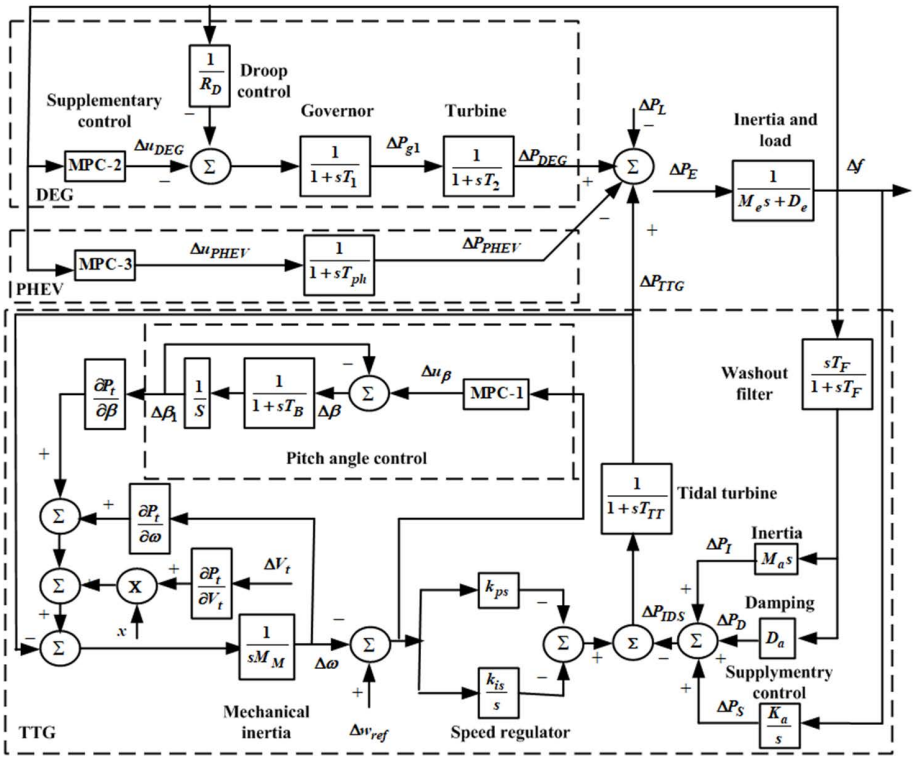

FIGURE 1. Single-area HPS model.

(a) Time-domain performance investigation of LFC of studied single-and two-area HPS models comprising of less explored combination formed using TTG, DEG, PHEVs, and conventional units are carried out.
(b) The optimal LFC performance is achieved using MPC, whose best design is accomplished utilizing QOHSA. The efficacy of QOHSA in tuning MPC is compared with other existing optimization algorithms.
(c) A comparative study on the performance of QOHSA tuned MPC and conventional controllers in regulating frequency is presented. The effect of model mismatch and noise on LFC performance is also investigated.
(d) The investigation is further extended to a two-area multi-machine HPS model.

This research study is organized into five sections. In Section 2, system modeling detail is presented. The proposed control method and mathematical problem formulation are briefed in Section 3. In Section 4, time domain-based simulation results are presented, and the study is summarized and concluded in Section 5.

II. STUDY SYSTEM MODELING

This section presents descriptions of TTG, DEG, and PHEVs as well as studied HPS models (see Fig. 1). Transfer function models of different DGs and HPS models are presented in the following subsections.

A. HPS MODELS

In the present work, a single-area HPS model comprising of five TTGs, one DEG, and PHEVs is considered and its linearized model is shown in Fig. 1 [16], [29]. In the studied HPS, each TTG of 1 MW capacity [15] and DEG of 5 MW capacity [10] are considered. PHEVs of 5 MW capacity (the total number of PHEVs are taken as 1000 with each having a capacity of 5 kW) are adopted for the simulation work [4]. In this system, the MPC approach is used for blade pitch angle control of TTGs, supplementary controller of DEG and power controller of PHEVs. Based on single-area HPS, a two-area HPS model is developed.

B. TTG SYSTEM

Block diagram of deloaded TTG with inertia, damping and supplementary controls are presented in Fig. 1. Mechanical power output (P_t) of TTG is calculated by (1)

$$P_t = 0.5\rho_t A_t V_t^3 C_{pt} \tag{1}$$

where, ρ_t refers to the density of water (in kg/m^3), A_t indicates swept-area by the turbine blades (in m^2), V_t is the tidal speed (in m/sec) and C_{pt} is the coefficient of performance. γ is the tip speed ratio and β is the blade pitch angle. C_{pt} and γ are expressed by (2) and (3), respectively [15]

$$C_{pt} = \left(\frac{c_1 c_2}{\gamma + c_6\beta} - \frac{c_1 c_7}{\beta^3 + 1} - c_1 c_3 \beta - c_1 c_4\right) \times \exp\left(\frac{-c_5}{\gamma + c_6\beta} + \frac{c_5 c_7}{\beta^3 + 1}\right) \tag{2}$$

$$\gamma = \omega R_t / V_t \tag{3}$$

where, R_t and ω are the radius (in m) and the rotational speed (in rad/sec) of the blades, respectively. $c_1 - c_7$ are

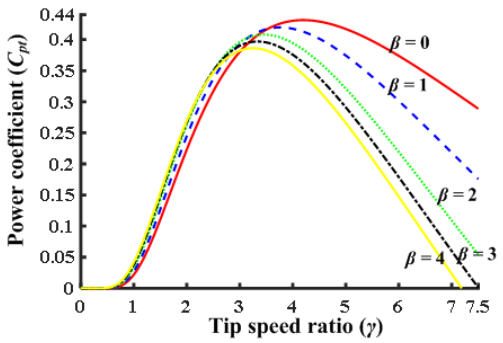

(a) Characteristics curves of C_{pt} versus γ at different values of β

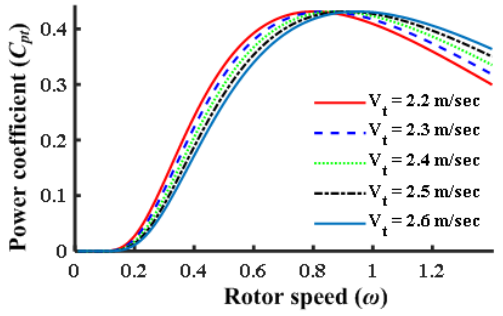

(b) Characteristics curves of C_{pt} versus ω at different values of V_t

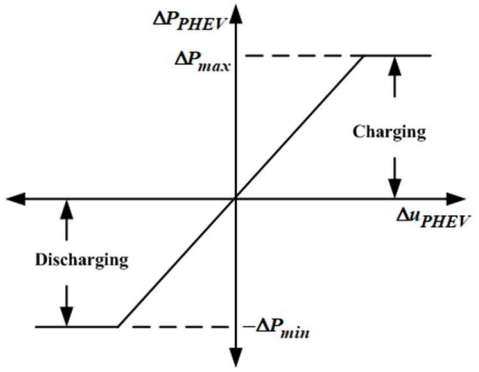

(c) Power output variation of PHEV using control signal

FIGURE 2. Characteristics curves.

the constant parameters taken from the work of [15], [16], [29], whose details are mentioned in the Appendix Section. Characteristics curves of C_{pt} versus γ at different values of and C_{pt} versus ω at varying values of V_t are portrayed in Fig. 2(a) and Fig. 2(b), respectively. The tidal power variation (ΔP_t) of TTG can be expressed by (4)

$$\Delta P_t = \Delta V_t \frac{\partial P_t}{\partial V_t} + \Delta\omega \frac{\partial P_t}{\partial \omega} + \Delta\beta \frac{\partial P_t}{\partial \beta} \tag{4}$$

where power output deviations $\partial P_t/\partial V_t$, $\partial P_t/\partial \omega$, and $\partial P_t/\partial \beta$ with respect to variation in tidal speed, turbine rotor speed, and blade pitch angle, respectively. The expression of $\partial P_t/\partial V_t$, $\partial P_t/\partial \omega$ and $\partial P_t/\partial \beta$ may be expressed by (5)-(9)

$$\frac{\partial P_t}{\partial V_t} = 1.5\rho_t A_t V_t^2 C_{pt} \tag{5}$$

$$\frac{\partial P_t}{\partial \omega} = 0.5\rho_t A_t V_t^3 \frac{\partial C_{pt}}{\partial \gamma}\frac{\partial \gamma}{\partial \omega} \tag{6}$$

$$\begin{aligned}\frac{\partial C_{pt}}{\partial \gamma}\frac{\partial \gamma}{\partial \omega} &= \exp\left(-\frac{c_5}{\gamma + c_6\beta} + \frac{c_5 c_7}{\beta^3+1}\right)\left(\left(\frac{R_t c_1}{V_t}\left(\frac{c_2}{\gamma + c_6\beta}\right.\right.\right.\\ &\quad \left.\left.\left. - \frac{c_2 c_7}{\beta^3+1} - c_3\beta - c_4\right)\left(\frac{c_5}{(\gamma + c_6\beta)^2}\right)\right)\right.\\ &\quad \left. + \left(\frac{-c_1 c_2}{(\gamma + c_6\beta)^2}\right)\right)\end{aligned} \tag{7}$$

$$\frac{\partial P_t}{\partial \beta} = 0.5\rho A_t V_t^3 \frac{\partial C_{pt}}{\partial \beta} \tag{8}$$

$$\begin{aligned}\frac{\partial C_{pt}}{\partial \beta} &= c_1 \exp\left(\frac{c_5 c_7}{\beta^3+1} - \frac{c_5}{\gamma + c_6\beta}\right)\\ &\quad \times \left(\left(\frac{c_5 c_6}{(\gamma + c_6\beta)^2} - \frac{3c_5 c_7 \beta^2}{(\beta^3+1)^2}\right)\right.\\ &\quad \times \left(-c_4 + \frac{c_2}{\gamma + c_6\beta} - \frac{c_2 c_7}{\beta^3+1} - c_3\beta\right)\\ &\quad \left. + \left(\frac{3c_2 c_7 \beta^2}{(\beta^3+1)^2} - \frac{c_2 c_6}{(\gamma + c_6\beta)^2} - c_3\right)\right)\end{aligned} \tag{9}$$

The parameters of TTG like turbine constant (T_T) and inertia (M_M) are calculated based on [15], [29] (see Appendix C), while blade-pitch time constant (T_B) is taken from [15]. Frequency-dependent power output (ΔP_{IDS}) of TTG (see Fig. 1) depends on inertia, damping and supplementary controls (here referred to as *IDS* control) having gain representation as M_a, D_a and K_a, respectively. *IDS* control is realized using a PID controller. In this paper, the value of M_a, D_a and K_a are taken as constant [16]. The power output variation of TTG (ΔP_{TTG}) is regulated by pitch angle control and it may cause power output to vary between the operating point at deloading to MPP. Pitch angle control is realized using the proposed method.

C. DEG SYSTEM

DEG contains two controllers (i.e., droop controller and supplementary controller) as shown in Fig. 1 [10]. Droop controller is also known as the primary control (i.e., used for quick action to a sudden change of load demand but fails to make frequency deviation to zero) and may be expressed as a proportional controller with a gain of $1/R_D$. The supplementary controller offset the steady-state error to zero. It acts more slowly than the primary control. In this work, the supplementary controller of DEG is realized using the proposed MPC.

D. PHEVs SYSTEM

The first-order transfer function of the PHEV model with the time delay (T_{ph}) is showcased in Fig. 1 [4]. The PHEV power output is the bi-directional charging and discharging from grid to vehicle and vehicle to grid (V2G), respectively. The change in PHEV power output (ΔP_{PHEV}) of V2G is regulated based on the control signal (u_{ph}) of the controller. The power output deviation of PHEV is expressed by (10) (see Fig. 2(c))

$$\Delta P_{PHEV} = \begin{cases} \Delta u_{ph}, & |\Delta u_{ph}| \le \Delta P_{max} \\ \Delta P_{max}, & \Delta u_{ph} > \Delta P_{max} \\ -\Delta P_{max}, & \Delta u_{ph} > -\Delta P_{max} \end{cases} \tag{10}$$

where P_{max} is the maximum power output of PHEV.

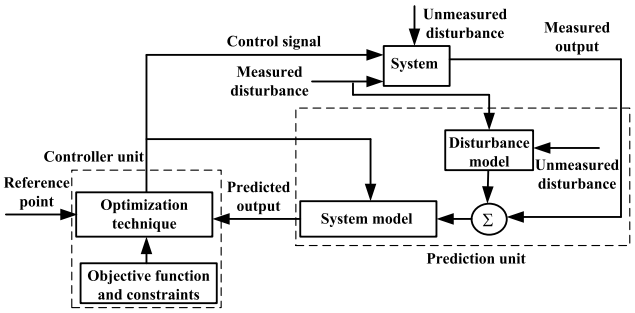

FIGURE 3. Generalized scheme of MPC [22].

III. MPC DESIGN

In this section, details on the studied MPC and its application for blade pitch angle control of TTG, supplementary control of DEG and power output control of PHEV are presented.

A. MPC METHOD

MPC employs a receding horizon concept in establishing a control sequence in order to assure closed-loop stability. MPC has two basic units, one is the prediction unit and the other one is the controller unit as shown in Fig. 3 [22]. MPC is based on explicit use of a prediction model of the system response to obtain the control actions by minimizing the objective function. Optimization objectives include minimization of the difference between the predicted and reference responses, and the control effort subjected to prescribed constraints (i.e. the optimization is subject to constraints on both manipulated and controlled variables and it is used to calculate the best set of future control action). In MPC, the control signal moves in such a way that the predicted output changes as per the reference point in an optimal manner. The MPC has the blend of both feed-forward and the feedback control features. The first one rejects most of the measured/unmeasured disturbances before affecting the system, while the second rejects the remainder disturbances. In this study, based on Fig. 3, three model predictive controllers are designed (see Fig. 1) indicated as MPC-1, MPC-2, and MPC-3 for DEG unit, PHEV unit and blade pitch control, respectively. Inputs to these MPCs are either the change in system frequency or speed of TTG turbine, which after being processed initiate the control actions to the respective blocks through controls referred as Δu_{DEG}, Δu_{PHEV}, and Δu_{β}.

A tractable MPC strategy must satisfy the constraints on the state of the system in the presence of uncertainty and control the plant optimally with respect to the performance index. The state of the system must be kept within the feasible set as much as possible. In this proposed work, tractable MPC strategy is implemented using the receding horizon principle.

MPC is designed as a discrete state-space model and, hence, the sampling period (T_s) is considered. At instant k, manipulated inputs may calculate a set of M (i.e., control horizon) values of input as $u(k+j-1)$(where, $j = 1, 2, \ldots, M$). Manipulated inputs are held constant between M and P (i.e., prediction horizon) values so that the predicted output reaches the reference point. MPC solves an optimization problem for finite future time steps at the current time. The finite impulse response of the system may be expressed by (11) [20]

$$y(m+1) = y(m) + A\sum_{j=0}^{n} \delta_j u(m-j) \tag{11}$$

where $y(m)$ is the manipulated output vector at time instance m, n is the number of impulse response coefficients, A is the interaction matrix, and δ_j is the coefficient number. δ_j may be expressed by (12)

$$\delta_j = h_{j+1} - h_j \tag{12}$$

where h_j is the scalar value such that h_jA is the jth impulse response coefficient matrix. To compute, the generalized MPC is defined by (13) [21]

$$\min_{u(m)\in M} \sum_{i=1}^{M} (y(m+i) - r(m+i))^T R(y(m+i) - r(m+i)) + (u(m) - u(m-1))^T Q(u(m) - u(m-1)) \tag{13}$$

where $r(m+i)$ is the reference trajectory, R and Q are the weighting factors. The state variable at the sampling instant $m+1$ for the state-space model with T_s may be expressed as

$$\begin{aligned} x(m+1) &= Ax(m) + Bu(m) + B_d d(m) \\ y(m) &= Cx(m) \end{aligned} \tag{14}$$

with the constraints given in (15)

$$\begin{aligned} u_{min}(m) &\le u(m) \le u_{max}(m) \\ y_{min}(m) &\le y(m) \le y_{max}(m) \end{aligned} \tag{15}$$

where B, B_d, and C are the coefficient matrices of appropriate dimensions. The values of set points, measured disturbances, and constraints are stated over a finite horizon of future sampling instants i.e. $m+1, m+2, \ldots, m+P$ along with controller computes M moves i.e. $m, m+1, \ldots, m+M$-1.

The proposed design is carried out employing the MPC toolbox of MATLAB software. It is to be noted that the choice of the sampling period (T_s), prediction horizon (P) and control horizon (M) are crucial to obtain a better performance of the MPC, hence, these parameters are optimized by employing the studied QOHSA.

B. BLADE PITCH ANGLE CONTROL OF TTG USING MPC

The MPC-based blade pitch angle control of TTG is realized (see Fig. 1) for smooth tidal power output. The inputs used for the suggested MPC are change in rotor speed ($\Delta\omega$) and change in reference point (Δw_{ref}) for generating manipulated control signal. The power output of TTG using MPC is expressed by (16)

$$\Delta P_{TTG}(m+1) = \Delta P_{TTG}(m) + A_{TTG}\sum_{j=0}^{n} \delta_j \Delta u_{\beta}(m-j) \tag{16}$$

where $\Delta P_{TTG}(m)$ and $\Delta u_\beta(m)$ are the deviations in power output of TTG and the manipulated input vector of blade pitch angle at instant m, respectively. A_{TTG} is the interaction matrix of TTG. The constraints of TTG are given in (17).

$$\begin{aligned} 0^\circ \le u_\beta \le 90^\circ \\ \left|\frac{\partial u_\beta}{\partial t}\right| \le 8^\circ/\text{sec} \end{aligned} \tag{17}$$

Since TTG system is represented by a linear mathematical model, the value of A_{TTG} is considered as 1.

C. SUPPLEMENTARY CONTROL OF DEG USING MPC

Supplementary controller of DEG realized using MPC is displayed in Fig. 1. The state-space model of the DEG can be expressed by (18)-(19)

$$\frac{\partial}{\partial t}\begin{bmatrix}\Delta P_{g1}\\ \Delta P_{DEG}\\ \Delta f\end{bmatrix} = \begin{bmatrix}-1/T_1 & 0 & -1/(T_1R_D)\\ 1/T_2 & -1/T_2 & 0\\ 0 & 1/M_e & -D_e/M_e\end{bmatrix} \times \begin{bmatrix}\Delta P_{g1}\\ \Delta P_{DEG}\\ \Delta f\end{bmatrix} + \begin{bmatrix}1/T_1\\ 0\\ 0\end{bmatrix}\Delta u_{DEG} \tag{18}$$

$$\Delta y = \begin{bmatrix}0 & 0 & 1\end{bmatrix}\begin{bmatrix}\Delta P_{g1}\\ \Delta P_{DEG}\\ \Delta f\end{bmatrix} + [0]\,\Delta u_{DEG} \tag{19}$$

where ΔP_{DEG} is the change in controlled power output, Δu_{DEG} is the output signal deviation of MPC, T_1 and T_2 are the time constants of governor and turbine, respectively, Δf is the frequency deviation, M_e and D_e are the equivalent inertia and damping coefficients of the studied system, respectively. The MPC used for DEG power output regulation is stated as

$$\Delta P_{DEG}(m+1) = \Delta P_{DEG}(m) + A_{DEG}\sum_{j=0}^{n}\sigma_j \Delta u_{DEG}(m-j) \tag{20}$$

where $A_{DEG} = [-1/T_1 \quad 0 \quad -1/(T_1R_D);\ 1/T_2 \quad -1/T_2 \quad 0;\ 0 \quad 1/M_e \quad -D_e/M_e]$ and $\Delta P_{DEG}(m)$ are the interaction matrix and the deviation in power output of DEG at instant m, respectively.

D. ACTIVE POWER OUTPUT CONTROL OF PHEV USING MPC

Power output control of PHEV using MPC is shown in Fig. 1. Referring closed loop structure of PHEV in Fig. 1, the transfer function of different blocks and related differential equations can be written as per (21)-(24)

$$\frac{\Delta P_{PHEV}}{\Delta u_{PHEV}} = \frac{1}{1+sT_{ph}} \tag{21}$$

$$\frac{\partial}{\partial t}(\Delta P_{PHEV}) = \frac{\Delta u_{PHEV}}{T_{ph}} - \frac{\Delta P_{PHEV}}{T_{ph}} \tag{22}$$

$$\frac{\Delta f}{\Delta P_{PHEV}} = \frac{-1}{M_e s + D_e} \tag{23}$$

$$\frac{\partial}{\partial t}(\Delta f) = -\frac{\Delta P_{PHEV}}{M_e} - \frac{D_e \Delta f}{M_e} \tag{24}$$

From (22) and (24), the state-space model of PHEV is defined by (25) and (26) [4], [21].

$$\frac{\partial}{\partial t}\begin{bmatrix}\Delta P_{PHEV}\\ \Delta f\end{bmatrix} = \begin{bmatrix}-1/T_{ph} & 0\\ -1/M_e & -D_e/M_e\end{bmatrix}\begin{bmatrix}\Delta P_{PHEV}\\ \Delta f\end{bmatrix} + \begin{bmatrix}1/T_{ph}\\ 0\end{bmatrix}\Delta u_{PHEV} \tag{25}$$

$$\Delta y = \begin{bmatrix}0 & 1\end{bmatrix}\begin{bmatrix}\Delta P_{PHEV}\\ \Delta f\end{bmatrix} + [0]\,\Delta u_{PHEV} \tag{26}$$

This state-space model of the PHEV is used for MPC calculations and it may be calculated as

$$\Delta P_{PHEV}(m+1) = \Delta P_{PHEV}(m) + A_{ph}\sum_{j=0}^{n}\tau_j \Delta u_{PHEV}(m-j) \tag{27}$$

where $\Delta P_{PHEV}(m)$ and $A_{ph} = [-1/T_{ph} \quad 0;\ -1/M_e \quad -D_e/M_e]$ are the power output deviation and the interaction matrix of PHEV at instant m, respectively.

E. TUNNING THE PARAMETERS OF MPCs

The values of the T_s, P, and M of MPCs associated with TTG, DEG and PHEVs are simultaneously tuned by QOHSA. The pseudo-code of the QOHSA is mentioned in [29]. In the present work, integral square error (ISE) is chosen as the objective function (referred to as the figure of demerit (FOD)) and is mathematically expressed by (28)

$$FOD = \int_0^t (\Delta f)^2 dt \tag{28}$$

where t is the simulation time (in sec). Performance indices like integral absolute error (IAE), integral time absolute error (ITAE) and integral time square error (ITSE) are also evaluated to verify the effectiveness of the proposed method further. In [16], more details of IAE, ITAE and ITSE are presented.

IV. SIMULATION RESULTS AND DISCUSSIONS

The optimal performance of the LFC of the studied single- and two-area HPS models (see Fig. 1 and Fig. 4) are examined using the proposed QOHSA tuned MPC through the time domain simulations in MATLAB^R. The studied models are developed using the SIMULINK toolbox, while the codes for QOHSA and other algorithms such as PSO, TLBO and GA are written in m file. Performance analysis of QOHSA tuned MPC-based LFC of the studied models are highlighted as different scenarios. Values of associated parameters of the investigated system are given in Appendix.

A. SCENARIO 1: QOHSA TUNED MPC-BASED LFC PERFORMANCE IN SINGLE-AREA HPS

In this scenario, a single-area HPS model comprising TTG, DEG, and PHEV is considered for the performance analysis

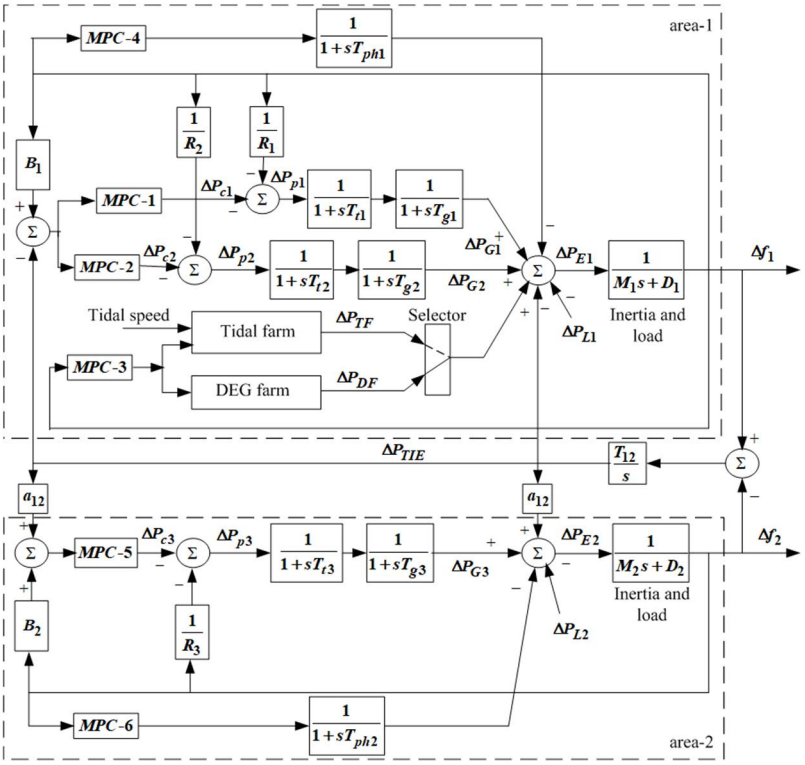

FIGURE 4. Two-area HPS model.

TABLE 1. Best chosen parameters of QOHSA and MPC (Scenario 1).

Technique	Value
QOHSA	HMS = 60, $HMCR$ = 0.4, J = 0.4, PAR^{min} = 0.45, PAR^{max} = 0.98, BW^{min} = 0.00005, BW^{max} = 50
GA	crossover probability (ρ_c) = 0.75, mutation probability (ρ_M) = 0.01
PSO	Inertial weight (W_{PSO}) = 0.6298, acceleration constants c_1 = 1 and c_2 = 1.3962
TLBO	teaching factor (tf) = 2
MPC	weights on manipulated variables (Q) = 1I, weights on manipulated variables rates = 0.1I, weights on output variables (R) = 1I

TABLE 2. Optimized parameters of the QOHSA, PSO, GA and TLBO tuned MPC with its constraint limit (Scenario 1).

Parameter	K_{mi}^{min}	K_{mi}^{max}	Algorithms used for MPC Tuning			
			QOHSA	GA	PSO	TLBO
M	1	5	2	2	2	3
P	5	15	14	10	9	10
T_s	0.01	1	0.0296	0.0411	0.0418	0.0321

of MPC-based LFC. In this model, TTGs are operated at a tidal speed of 2.4 m/sec with an initial blade pitch angle of 3° representing 15 % deloaded operation (represented by $x = 0.15$ (see Fig. 1)). The system under consideration is in p.u. with base power considered as 5 MW. Four different analyses are carried out in this scenario including (a) to prove the tuning efficiency of adopted QOHSA, (b) to prove superior performance of QOHSA tuned MPC, (c) to analyze the LFC performance employing QOHSA tuned MPC with increased load demands, and (d) to examine impact of model mismatch and noise on LFC performance.

1) PERFORMANCE ANALYSIS OF QOHSA TUNED MPC

The studied model is subjected to 1% step load perturbation (SLP) (ΔP_L) i.e., 0.05 MW at $t = 2$ sec. The best values of the parameters associated with QOHSA, PSO, TLBO, and GA are presented in Table 1. QOHSA, PSO, TLBO, and GA are used one by one to tune the parameters associated with MPC (i.e., M, P and T_s) for getting the optimal performance of the LFC loop which are presented in Table 2. In Table 2, K_{mi}^{min} and K_{mi}^{max} are the minimum and the maximum range of the parameters associated with MPC. The comparative transient response of frequency deviation (Δf) and convergence profiles obtained under QOHSA, PSO, TLBO, and GA tuned MPC is presented in Fig. 5. It can be inferred from Fig. 5 that the QOHSA tuned MPC gives better frequency regulation and the minimum FOD values than the other counterparts. Hence, for the rest of the study, QOHSA will be adopted.

2) COMPARATIVE PERFORMANCE ANALYSIS OF QOHSA TUNED MPC AND PID CONTROLLER

In this section, the superiority of the proposed QOHSA tuned MPC is established. The results obtained utilizing QOHSA tuned MPC is compared with that of QOHSA tuned PID controller. The optimally designed controller parameters of

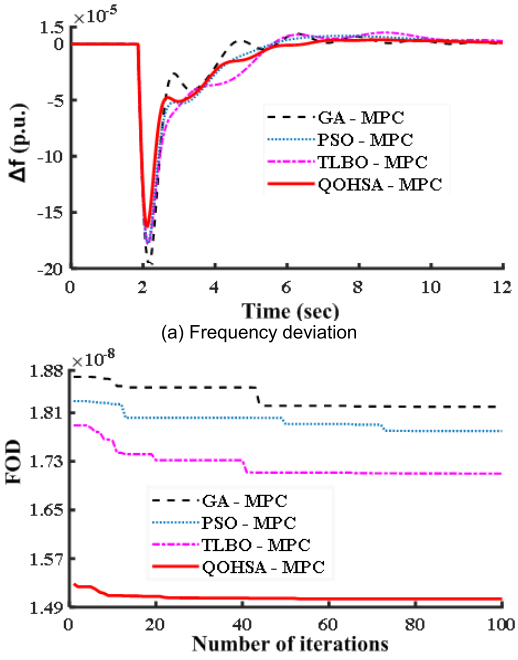

FIGURE 5. Scenario 1: Comparative profiles obtained employing GA, PSO, TLBO and QOHSA tuned MPCs.

TABLE 3. Optimized parameters of QOHSA tuned PID controller (Scenario1).

Controller's parameters	Controller application		
	Blade pitch	DEG	PHEV
K_P	2.79	16.20	5.93
K_I	0.01	5.20	10.39
K_D	15.74	5.80	5.51

the QOHSA tuned PID controller are taken from Table 3. The comparative response profiles of frequency deviation and convergence curve of FOD are plotted in Fig. 6(a) and Fig. 6(b), respectively. From the simulated results (refer to Fig. 6), it can be inferred that the maximum frequency deviation and value of convergence curve obtained are the lowest for the proposed method in comparison to QOHSA tuned PID controllers. Frequency deviation with the proposed method is better in terms of peak overshoot, undershoot and settling time as shown in Fig 6(a). The value of FOD and other performance indices (considered as ITSE, IAE and ITAE) are presented in Table 4 and it is observed that the obtained value of FOD and performance indices are the minimum with the proposed method. From Fig. 6 and Table 4, it may be concluded that the performance of the proposed method is the best. Based on the above results, for further studies, QOHSA tuned MPC will be utilized.

3) PERFORMANCE ANALYSIS OF LFC EMPLOYING QOHSA TUNED MPC WITH INCREASED LOAD DEMANDS

In this scenario, different steps of load demand are applied at $t = 2$ sec and the optimally designed proposed controller

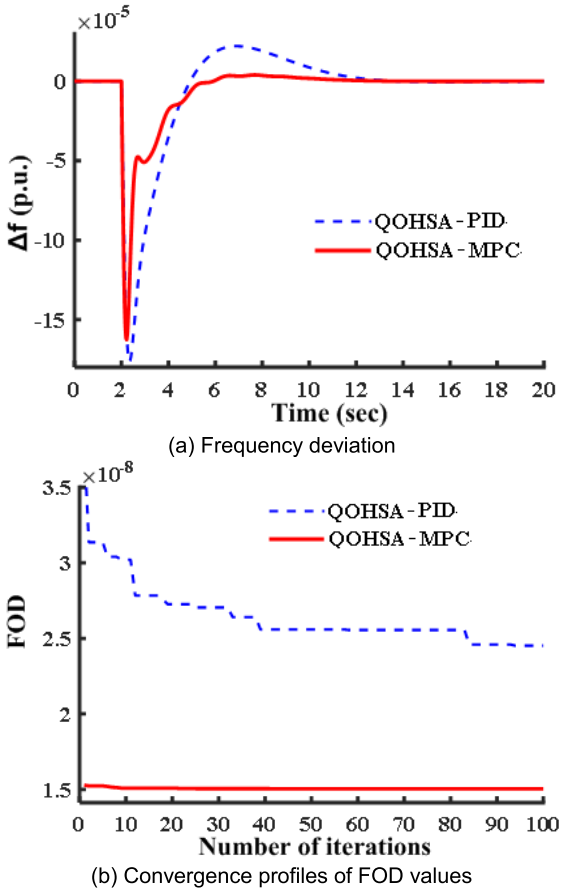

FIGURE 6. Scenario 1: Comparative profiles obtained under the action of QOHSA-PID and QOHSA-MPC.

TABLE 4. FOD values and performance indices obtained for the studied single-area HPS with 1% SLP (Scenario 1).

Studied topology	FOD ($\times 10^{-8}$)	Performance indices		
		ITSE ($\times 10^{-8}$)	IAE ($\times 10^{-4}$)	ITAE
QOHSA-PID	2.4520	7.2761	3.0277	0.0014
QOHSA-MPC	1.5037	2.6027	1.4788	0.0005

parameters are taken from Table 2. The two different cases of simulation are carried out in this analysis which corresponds to 1% and 2% increase in load demand, respectively. The comparative response profiles of frequency deviations, the generated power output of TTGs, blade pitch angle variation, power output generated from DEG, power output generated from PHEVs, and output control signals of MPC-1, MPC-2, and MPC-3 (used for TTG, DEG, and PHEVs, respectively) obtained under the two cases of load scenarios are presented in Figs. 7 and 8. These response profiles are obtained under the proposed control method. It can be observed from Fig. 7(a) that following SLP, the maximum deviation of response profiles and settling time are observed in the case of a 2% increase in load demand. In other words, if load demand is increased then the maximum deviation in response profiles of the system is also increased. However, it is shown that

in the presence of proposed method, frequency deviation is settled down very quickly and oscillation of signals is damped out very fast under different load disturbance. This is due to the permanent participation of TTGs (see Fig. 7(b)) by changing blade pitch angle (see Fig. 7(c)), supplementary controller of DEG (see Fig. 7(d)) and power controller of PHEVs (see Fig. 7(e)). The power output of TTGs varies smoothly and rises continuously up to steady-state value. The smooth variation in power output from TTGs is noticed due to the available reserved power margin of the TTGs. While, at the time, when load demand increases, power output variation from DEG reaches its peak value very quickly to compensate for the load demand (see Fig. 7(d)). Similarly, PHEVs (see Fig. 7(e)) respond swiftly to compensate for load demand and aid in frequency regulation, effectively. It is observed that using the proposed QOHSA tuned MPC for blade pitch control along with the associated inertia, damping and supplementary controls (i.e., IDS Control), the participation of TTGs decreases the burden on DEG and PHEVs to enhance the system performance under different load disturbances.

Figs. 8(a)-(c) portray the output control signals Δu_β, Δu_{DEG} and Δu_{PHEV} of the MPCs associated with TTGs (i.e., MPC-1), DEG (i.e., MPC-2) and PHEVs (i.e., MPC-3), respectively.

4) EFFECT OF MODEL MISMATCH AND NOISE ON LFC PERFORMANCE

The accuracy of the power system model plays a vital role in assessing the performance of MPC. The model-plant mismatch may have a substantial effect on the process. In [28], effect of four types of mismatch (such as gain, reverse gain, time constant, and time delay mismatches) on MPC performance in a process industry has been investigated. In this work, we consider only time constant mismatch as a kind of model mismatch in the studied power system. For this, only the time constant of DEG (i.e., T_1) is chosen and it is varied by $\pm 25\%$ and $\pm 50\%$ from their nominal values, taking one at a time. Fig. 9 gives the frequency deviation response of the QOHSA-based MPC for a 1% SLP. Table 5 presents the value of the maximum frequency deviation obtained under different values of the time constant of DEG. The response obtained reveals that time constant mismatch has a negligible impact on the performance of QOHSA tuned MPC used for the LFC task.

Further, the dynamic performance of the studied power system has been simulated under load disturbance with white noise. Typically, white noise exists in the load disturbances owing to continuous switching operations of the consumer's equipment. The considered load disturbances with white noise have been displayed in Fig. 10(a). SLP of 1% occurs at $t = 2$ sec. The response profiles of frequency deviations, power output generated from TTGs, power output generated from DEG, power output generated from PHEVs, and control signals are presented in Figs. 10 and 11. It can be observed

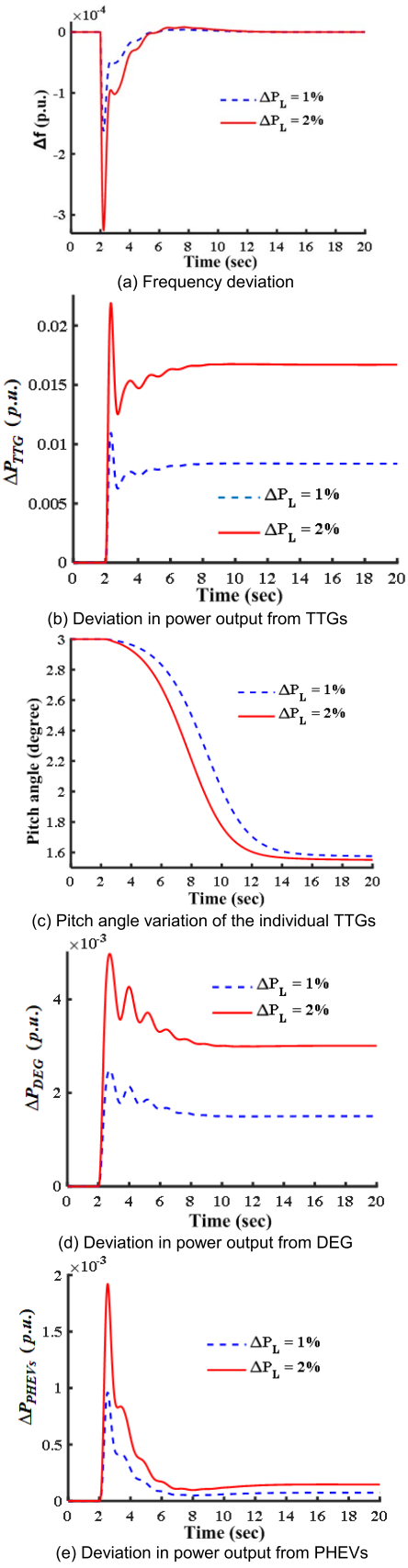

FIGURE 7. Response profiles obtained under load deviation pertaining to Scenario 1.

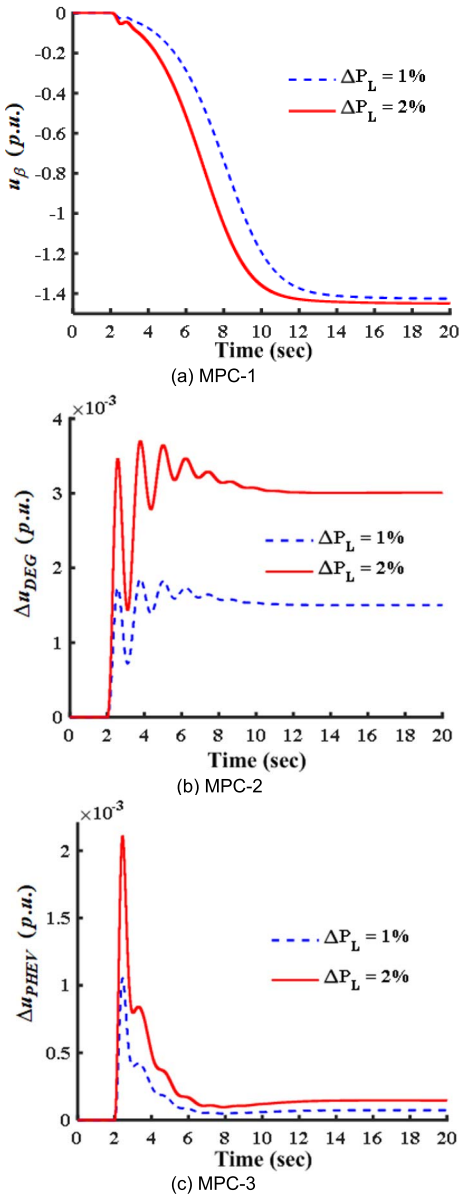

FIGURE 8. Profiles of control signal obtained under load deviation pertaining to Scenario 1.

that the QOHSA-based MPC may handle noise very effectively with some minor oscillations in the various profiles shown in Figs. 10 and 11.

B. SCENARIO 2: QOHSA TUNED MPC-BASED LFC PERFORMANCE IN TWO-AREA HPS

To confirm the given investigation and to corroborate the efficacy of the proposed MPC method, two-area multi-machine HPS is considered (see Fig. 4). The data of conventional generators are shown in Table 6, and the values of other parameters of two-area HPS are presented in Appendix.The values of the parameters of the MPCs are mentioned in Table 2. In the two-area HPS model, a tidal farm of 200 MW capacity is considered and is achieved by aggregating 200 TTG units of 1 MW capacity each. A DEG farm of 200 MW

TABLE 5. Effect of the maximum frequency deviation under mismatch variation of time constant values of DEG (Scenario 1).

Mismatch variation (in %)	New time constant T_1 (in sec)	Maximum frequency deviation (in p.u.)
0	0.1 (Nominal value)	-1.6272×10^{-4}
-25	0.075	-1.6262×10^{-4}
+25	0.125	-1.6393×10^{-4}
-50	0.05	-1.6122×10^{-4}
+50	0.15	-1.6443×10^{-4}

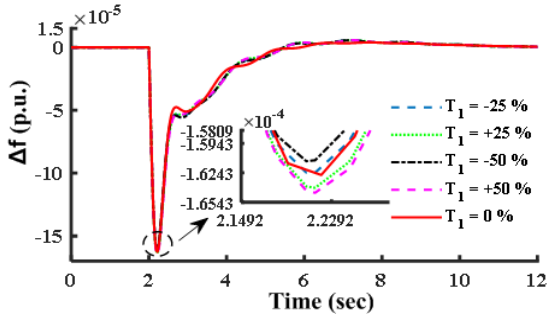

FIGURE 9. Frequency deviation obtained under different time constant values of DEG pertaining to Scenario 1.

TABLE 6. Parameters of generators of two-area HPS model (Scenario 2).

Generator	Rating (MW)	R_i (Hz/p.u. MW)	T_i (sec)	T_g (sec)
G_1	800	2.4	0.36	0.06
G_2	1000	2.4	0.4	0.08
G_3	1000	2.4	0.4	0.08

capacity is considered and is accomplished by aggregating 40 numbers (each of 5 MW capacity) of DEGs. PHEVs of 1000 MW capacity are considered and this is realized by aggregating 200000 PHEVs (each PHEV of 5 kW capacity).

Two areas (denoted as area-1 and area-2) are of 2000 MW and 1000 MW capacities, respectively. The area-1 consists of a tidal farm, a DEG farm, PHEVs and two conventional generating units(referred to as G1 and G2). The area-2 consists of conventional generating unit(i.e., G3) and PHEVs. In this scenario, the system under consideration is in p.u. with a base power of 2000 MW. Similar to Scenario 1, a step increase in load demand of 1% i.e., 20 MW is applied in this scenario in area-1 at $t = 2$ sec. Three different cases have been considered for this scenario and these are represented as follows:

Case(a): Area-1 is comprised of G1, G2, a tidal farm and PHEVs. In this case, frequency support from a tidal farm is considered zero (i.e., tidal farm operates at MPP).

Case(b): Area-1 is comprised of G1, G2, a DEG farm and PHEVs.

Case(c): Area-1 is comprised of G1, G2, a tidal farm and PHEVs. In this case, a tidal farm permanently participates in frequency regulation.

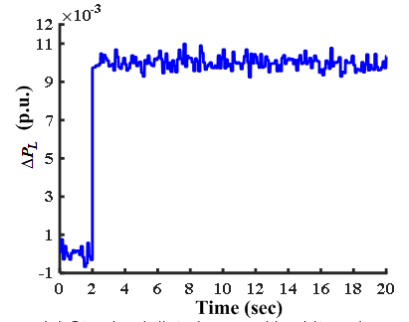

(a) Step load disturbance with white noise

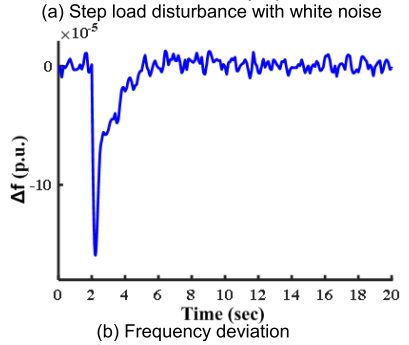

(b) Frequency deviation

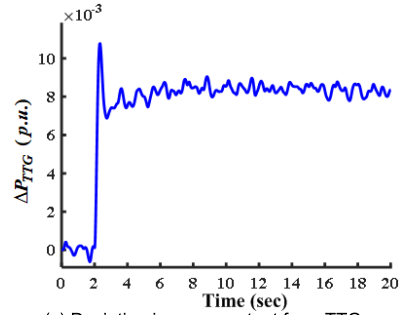

(c) Deviation in power output from TTGs

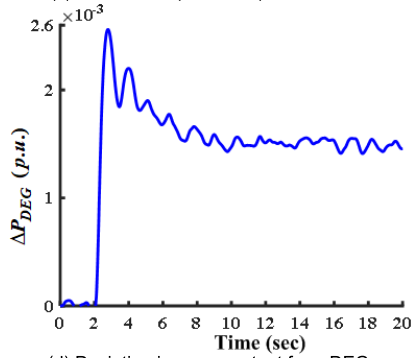

(d) Deviation in power output from DEG

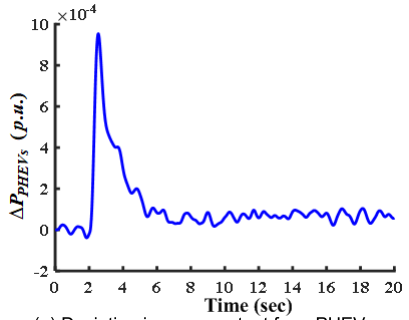

(e) Deviation in power output from PHEVs.

FIGURE 10. Response profiles obtained under load deviation pertaining to Scenario 1.

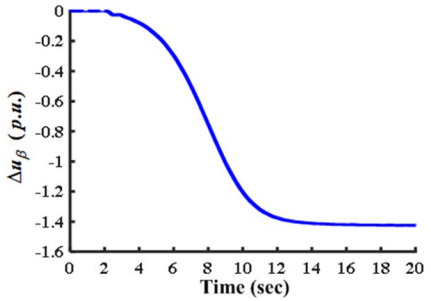

(a) MPC-1

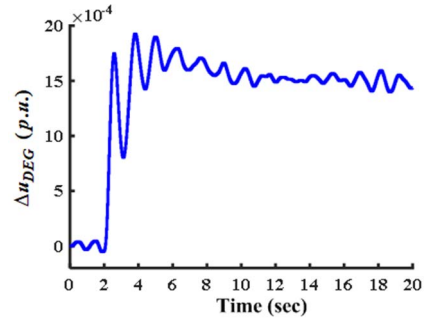

(b) MPC-2

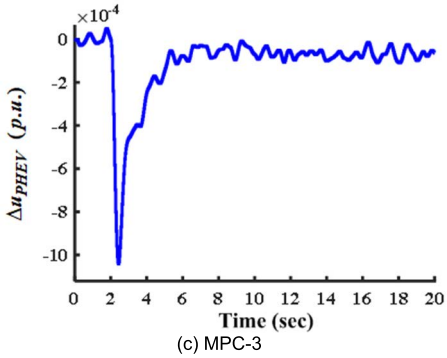

(c) MPC-3

FIGURE 11. Response profiles of control signal obtained under load deviation pertaining to Scenario 1.

In Fig. 12, the profiles of frequency deviation in area-1 (Δf_1), area-2 (Δf_2) and tie-line power deviation (ΔP_{TIE}) are presented. In Case(a), it is found that deviation in response profiles is the maximum due to zero power shared from the tidal farm, and so all the power-sharing burden goes to G1, G2, and PHEVs to compensate for the increase in load demand. In Case(b), it is shown that the maximum response profile deviations are decreased in comparison to Case(a). However, the response profile deviations are very high and have a large settling time. By using the proposed MPC method in Case(c), the tidal farm power output is changed at a fast pace for a particular variation in load demand. This quick action provides the minimum frequency deviation. Permanent participation with a steady-state value of power output from a deloaded tidal farm is due to its available active power reserve generated by cutting the blade pitch angle. Furthermore, it has also helped to decrease the burden on conventional generating units and PHEVs. It is shown in

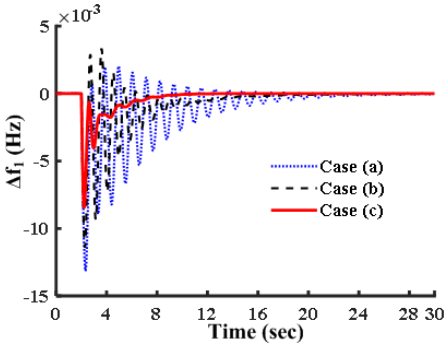

(a) Δf_1

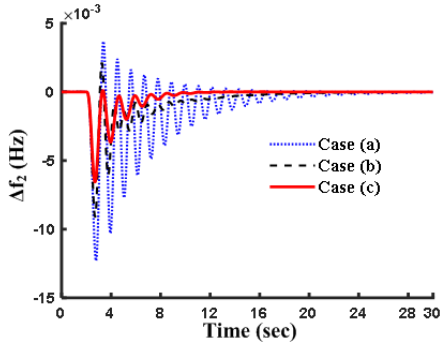

(b) Δf_2

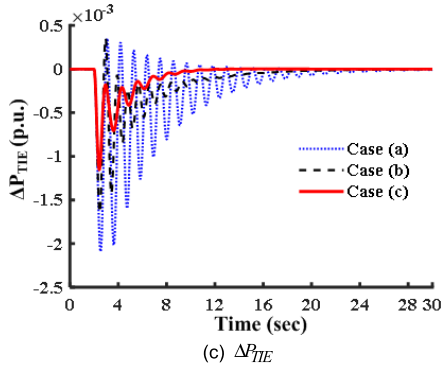

(c) ΔP_{TIE}

FIGURE 12. Response profiles obtained under step load deviation pertaining to Scenario 2.

Fig. 12 that the response profile deviations are better in terms of peak overshoot, undershoot, and settling time compared to Case(a) and Case(b). It is concluded from Case(c) that replacing the DEG farm with the tidal farm is a viable solution to improve the performance of LFC.

To study the robustness of the proposed method in a two-area power system, random variations in load demand (shown in Fig. 13(a)) are applied to area-1. The above-mentioned three different cases are implemented again. The comparative response profiles of Δf_1, Δf_2 and ΔP_{TIE} are presented in Figs. 13(b)-(d), respectively. It can be inferred from Figs. 13(b)-(d) that the proposed scheme with Case(c) performs better in comparison to the other cases (i.e., Case(a) and Case(b)). Moreover, the proposed method in Case(c) renders permanent participation of TTG and, thereby, diminishes the burden on conventional generators and PHEVs.

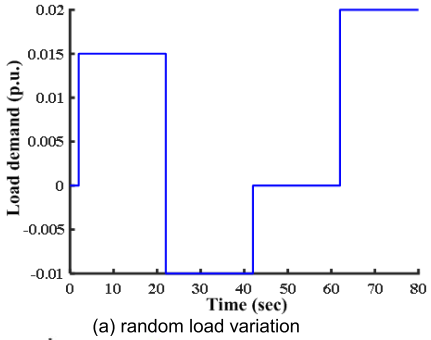

(a) random load variation

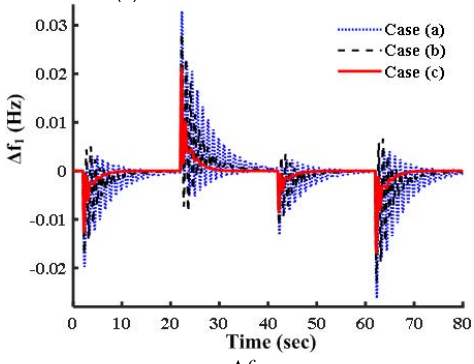

(b) Δf_1

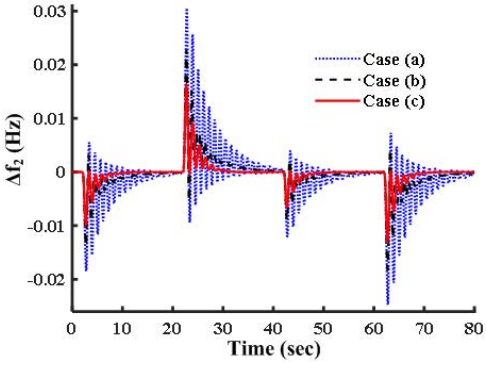

(c) Δf_2

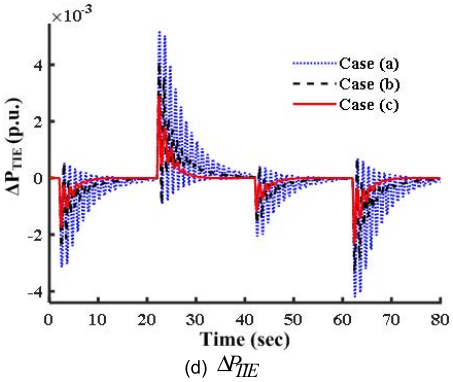

(d) ΔP_{TIE}

FIGURE 13. Profiles of random load variation and response profiles obtained under load deviation pertaining to Scenario 2.

V. CONCLUSION

In this paper, QOHSA tuned MPC is proposed and its performance on LFC of TTG, DEG, PHEVs, and conventional units assisted single- and two-area HPS models are analysed.

Firstly, QOHSA performance over other algorithms in tuning MPC is carried out, followed by a superiority test of QOHSA tuned MPC over QOHSA tuned conventional PID controllers. The performance of QOHSA tuned MPCs (associated with different DGs and other conventional units of the studied HPS models) in frequency regulation following different load perturbations is deeply analysed. Results reveal that TTG successfully participates in frequency regulations task through inertia, damping, and supplementary controls to alleviate generation-load mismatch along with other units in both the studied HPS models. The simulation results demonstrate that the proposed method yields a desirable performance and the power output from the TTG(s) positively impacts system stability. Further, the effect of model-mismatch and noise on MPC-based LFC performance is also investigated. In addition to the above-presented analysis (a) the performance of the proposed technique in TTG-assisted real power system model like 10-machine 39-bus New England power system may be explored, (b) new state-of-the-art optimization algorithms or the concept of hybrid optimization algorithms with MPC may be employed for the optimal design, and (c) hybrid approach comprising features of traditional solvers, metaheuristics/evolutionary algorithms, and MPC may be explored.

APPENDIX A
ABBREVIATIONS

DEG: Diesel Engine Generator; DGs: Distributed Generators; FOD: Figure of Demerit; GA: Genetic Algorithm; HPS: Hybrid Power System; IAE: Integral Absolute Error; ISE: Integral Square Error; ITAE: Integral Time Absolute Error; LFC: Load Frequency Control; MPC: Model Predictive Control; TLBO: Teaching Learning Based Optimization; MPP: Maximum Power Point; PHEV: Plug-in Hybrid Electric Vehicles; PID: Proportional Integral Derivative; PSO: Particle Swarm Optimization; QOHSA: Quasi-Oppositional Harmony Search Algorithm; TTG: Tidal Turbine Generator; V2G: Vehicle to Grid; WTG: Wind Turbine Generator.

APPENDIX B
VARIOUS HPS PARAMETERS

The various parameters of TTG, DEG, PHEVs, inertia and load used in the studied HPS models are as follows [10], [4], [15], [16], [29]

TTG:	Rated rotor speed (ω_r) = 13 rpm, V_{tr} = 2.4 m/sec, R_t = 11.5 m, rotor blades = 3, M_M = 0.3878 sec, T_B = 0.01 sec, T_{TT} = 0.08 sec, T_F = 6 sec, c_1 = 0.18, c_2 = 85, c_3 = 0.38, c_4 = 10.2, c_5 = 6.2, c_6 = 0.025, c_7 = -0.043, k_{ps} = 0.005, k_{is} = 0.006, M_a = 148.16, D_a = 149.87, K_a = 70.1, ρ_t = 1027 kg/m^3 , $A_t = \pi R_t^2$, Δw_{ref} = 0, tidal speed variation (ΔV_t) = 0
DEG:	Single-area: T_1 = 0.1 sec, T_2 = 0.25 sec, R_D = 0.04 p.u. Hz/p.u. MW
PHEVs:	Single-area: T_{ph} = 1 sec, ΔP_{PHEVs} limits: ± 5 MW, Two-area: T_{ph1} = T_{ph2} = 1 sec, ΔP_{PHEVs} limits: ± 1000 MW
Inertia and load:	Single-area: f = 50 Hz, M_e = 10 sec, D_e = 0.6 p.u. MW/p.u. Hz, Two-area: M_1 = M_2 = 0.1667 p.u. sec, D_1 = D_2 = 0.0084 p.u. MW/Hz, B_1 = B_2 = 0.425 p.u. MW/Hz, a_{12} = -2, T_{12} = 0.545 p.u. MW, P_{tiemax} = 200 MW, $\delta_1 - \delta_2$ = 30°

APPENDIX C
CALCULATION TTG PARAMETERS

Considering the design parameters of 1 MW TTG given below:

Rotor radius (R_t) = 11.5 m, Number of rotor blades = 3, Blade length = 10.6 m, Rotor position = upstream, Rotor inertia (J_r) = 110688 kgm^2, Rotor blade inertia (J_b) = 11986 kgm^2, Generator rotor inertia (J_g) = 86700 kgm^2, ρ = 1027 kgm^3, A_t = πR_t^2= 415 m^2, S = 1 MW, Rated torque (T_r) = 734753 Nm, following calculations are made:

Calculation of $M_M = 2H_{TTG}$: The values of H_{TTG} (in sec) is calculated as $0.5Jw_r^2/S$. The value of J is calculated as $J_r + J_g + J_b$ and the value of w_r (in rad/sec) is calculated as $2\pi\omega_r/60 = 1.361$. The value of H_{TTG} is calculated (using the formula $0.5(J_r + J_g + J_b)\omega_r^2/S$) as 0.1939 sec. Finally, the value of M_M is 0.3878 sec.

Calculation of T_{TT}: The value of T_{TT} (in sec) is calculated as $\frac{J\omega_r}{3T_r} = 0.08$ sec.

REFERENCES

[1] A. Baruah, M. Basu, and D. Amuley, "Modeling of an autonomous hybrid renewable energy system for electrification of a township: A case study for sikkim, India," *Renew. Sustain. Energy Rev.*, vol. 135, Jan. 2021, Art. no. 110158.

[2] M. Shivaie, M. Mokhayeri, M. Kiani-Moghaddam, and A. Ashouri-Zadeh, "A reliability-constrained cost-effective model for optimal sizing of an autonomous hybrid solar/wind/diesel/battery energy system by a modified discrete bat search algorithm," *Sol. Energy*, vol. 189, pp. 344–356, Sep. 2019.

[3] S. Li, Y. Li, and T. Li, "An autonomous flexible power management for hybrid AC/DC microgrid with multiple subgrids under the asymmetric AC side faults," *Int. J. Electr. Power Energy Syst.*, vol. 142, Nov. 2022, Art. no. 107985.

[4] S. Vachirasricirikul and I. Ngamroo, "Robust LFC in a smart grid with wind power penetration by coordinated V2G control and frequency controller," *IEEE Trans. Smart Grid*, vol. 5, no. 1, pp. 371–380, Jan. 2014.

[5] J. Mishra, P. K. Behera, M. Pattnaik, and S. Samanta, "An efficient supervisory power management scheme for a wind–battery-assisted hybrid autonomous system," *IEEE Syst. J.*, early access, Jun. 20, 2022, doi: 10.1109/JSYST.2022.3178632.

[6] P. Lin, C. Jin, J. Xiao, X. Li, D. Shi, Y. Tang, and P. Wang, "A distributed control architecture for global system economic operation in autonomous hybrid AC/DC microgrids," *IEEE Trans. Smart Grid*, vol. 10, no. 3, pp. 2603–2617, May 2018.

[7] V. Gholamrezaie, M. G. Dozein, H. Monsef, and B. Wu, "An optimal frequency control method through a dynamic load frequency control (LFC) model incorporating wind farm," *IEEE Syst. J.*, vol. 12, no. 1, pp. 392–401, Mar. 2018.

[8] T. Senjyu, R. Sakamoto, N. Urasaki, T. Funabashi, H. Fujita, and H. Sekine, "Output power leveling of wind turbine generator for all operating regions by pitch angle control," *IEEE Trans. Energy Convers.*, vol. 21, no. 2, pp. 467–475, Jun. 2006.
[9] G. Somnath, T. Mahto, and V. Mukherjee, "Integrated frequency and power control of an isolated hybrid power system considering scaling factor based fuzzy classical controller," *Swarm Evol. Comput.*, vol. 32, pp. 184–201, Feb. 2017.
[10] K. V. Vidyanandan and N. Senroy, "Primary frequency regulation by deloaded wind turbines using variable droop," *IEEE Trans. Power Syst.*, vol. 28, no. 2, pp. 837–846, May 2013.
[11] M. Tarkeshwar and V. Mukherjee, "Quasi-oppositional harmony search algorithm and fuzzy logic controller for load frequency stabilisation of an isolated hybrid power system," *IET Gener., Transmiss. Distrib.*, vol. 9, no. 5, pp. 427–444, Apr. 2015.
[12] M. Takagi, H. Yamamoto, K. Yamaji, K. Okano, R. Hiwatari, and T. Ikeya, "Load frequency control method by charge control for plug-in hybrid electric vehicles with LFC signal," *IEEJ Trans. Power Energy*, vol. 129, no. 11, pp. 1342–1348, 2009.
[13] H. Liu, Z. Hu, Y. Song, and J. Lin, "Decentralized vehicle-to-grid control for primary frequency regulation considering charging demands," *IEEE Trans. Power Syst.*, vol. 28, no. 3, pp. 3480–3489, Aug. 2013.
[14] A. G. Bryans, B. Fox, P. A. Crossley, and M. O'Malley, "Impact of tidal generation on power system operation in Ireland," *IEEE Trans. Power Syst.*, vol. 20, no. 4, pp. 2034–2040, Nov. 2005.
[15] B. Whitby and C. E. Ugalde-Loo, "Performance of pitch and stall regulated tidal stream turbines," *IEEE Trans. Sustain. Energy*, vol. 5, no. 1, pp. 64–72, Jan. 2014.
[16] A. Kumar and G. Shankar, "Quasi-oppositional harmony search algorithm based optimal dynamic load frequency control of a hybrid tidal–diesel power generation system," *IET Gener., Transmiss. Distrib.*, vol. 12, no. 5, pp. 1099–1108, Mar. 2018.
[17] S. M. Asanova, M. K. Safaraliev, S. E. Kokin, S. A. Dmitriev, K. Arfan, T. Z. Zhabudaev, and T. K. Satarkulov, "Optimization of the structure of autonomous distributed hybrid power complexes and energy balance management in them," *Int. J. Hydrogen Energy*, vol. 46, no. 70, pp. 34542–34549, Oct. 2021.
[18] H. Shayeghi, H. A. Shayanfar, and A. Jalili, "Load frequency control strategies: A state-of-the-art survey for the researcher," *Energy Convers. Manage.*, vol. 50, no. 2, pp. 344–353, Feb. 2009.
[19] K. S. Holkar and L. M. Wanghmare, "An overview of model predictive control," *Int. J. Control Autom.*, vol. 3, no. 4, pp. 47–64, 2010.
[20] J. L. Garriga and M. Soroush, "Model predictive control tuning methods: A review," *Ind. Eng. Chem. Res.*, vol. 49, no. 8, pp. 3505–3515, Apr. 2010.
[21] J. Pahasa and I. Ngamroo, "Coordinated control of wind turbine blade pitch angle and PHEVs using MPCs for load frequency control of microgrid," *IEEE Syst. J.*, vol. 10, no. 1, pp. 97–105, Mar. 2016.
[22] M. Elsisi, M. Soliman, M. A. S. Aboelela, and W. Mansour, "Bat inspired algorithm based optimal design of model predictive load frequency control," *Int. J. Electr. Power Energy Syst.*, vol. 83, pp. 426–433, Dec. 2016.
[23] D. Izci, S. Ekinci, E. Eker, and M. Kayri, "Augmented hunger games search algorithm using logarithmic spiral opposition-based learning for function optimization and controller design," *J. King Saud Univ. Eng. Sci.*, Mar. 2022, doi: 10.1016/j.jksues.2022.03.001.
[24] D. Izci, S. Ekinci, E. Eker, and L. Abualigah, "Opposition-based arithmetic optimization algorithm with varying acceleration coefficient for function optimization and control of FES system," in *Proc. Int. Joint Conf. Adv. Comput. Intelli.*, 2022, pp. 283–293.
[25] S. Ekinci, D. Izci, E. Eker, and L. Abualigah, "An effective control design approach based on novel enhanced Aquila optimizer for automatic voltage regulator," *Arti. Intelli. Rev.*, vol. 1, no. 1, pp. 1–32, 2022.
[26] H. R. Tizhoosh, "Opposition based learning: A new scheme for machine intelligence," in *Proc. Int. Conf. Comp. Intell. Model Control Autom.*, 2005, pp. 695–701.
[27] C. K. Shiva and V. Mukherjee, "A novel quasi-oppositional harmony search algorithm for AGC optimization of three-area multi-unit power system after deregulation," *Eng. Sci. Technol., Int. J.*, vol. 19, no. 1, pp. 395–420, Mar. 2018.
[28] A. I. Nafsun and N. Yusoff, "Effect of model-plant mismatch on MPC controller performance," *J. Appl. Sci.*, vol. 11, no. 21, pp. 3579–3585, Oct. 2011.
[29] A. Kumar and G. Shankar, "Optimal load frequency control in deloaded tidal power generation plant-based interconnected hybrid power system," *IET Renew. Power Gen.*, vol. 12, no. 16, pp. 1864–1875, 2018.

AKSHAY KUMAR received the B.Tech. degree in electrical and electronics engineering and the M.Tech. degree in electrical engineering from KIIT University, Odisha, India, in 2013 and 2015, respectively, and the Ph.D. degree in electrical engineering from IIT (ISM), Jharkhand, India, in 2021. Currently, he is working as Postdoctorate Fellow with the National Sun Yat-sen University, Taiwan. His research interests include power system optimization techniques, renewable energy, and FACTS devices.

NEETU KUMARI received the B.E. degree in electrical and electronics engineering from the Birla Institute of Technology, Mesra, India, in 2014, and the M.Tech. degree in industrial electronics from the National Institute of Technology (NIT), Rourkela, India, in 2017. She is currently pursuing the Ph.D. degree with the Department of Electrical Engineering, IIT (ISM) Dhanbad, India. Her main research interests include automatic generation control, cyber security of power systems, and application of data science for cyber-attack detection.

GAURI SHANKAR (Member, IEEE) received the B.E. degree in electrical and electronics engineering from the Birla Institute of Technology (BIT), Mesra, Ranchi, in 2003, the M.Tech. degree in energy studies from IIT Delhi, in 2005, and the Ph.D. degree in electrical engineering from IIT (ISM) Dhanbad, in 2016. He started his teaching career as a Lecturer with the School of Engineering, University of Petroleum and Energy Studies, Dehradun, in 2005. He worked as an Assistant Professor with the Department of Electrical Engineering, North Eastern Regional Institute of Science and Technology (NERIST), a deemed university under MHRD, GoI, Itanagar, Arunachal Pradesh, from 2006 to 2010. He joined IIT (ISM) Dhanbad, in 2010, where he is currently working as an Assistant Professor with the Department of Electrical Engineering. He has several years of teaching experience. He is an active member of many journals, publishers, and conferences as a reviewer or an organizer. He has authored or coauthored over 50 publications, including journal articles, monographs, book chapters, and conference papers of repute. His research interests include power system operation and control, distributed generation, power quality issues in microgrid, and soft computing techniques.

RAJVIKRAM MADURAI ELAVARASAN received the B.E. degree in electrical and electronics engineering from Anna University, Chennai, India, and the M.E. degree (Hons.) in power system engineering from Thiagarajar College of Engineering, Madurai, India. He is currently pursuing the Ph.D. degree with the School of Information Technology and Electrical Engineering, University of Queensland, Australia. He was a Technical Operations Associate with the IBM Global Technology Services Division. He was an Assistant Professor with the Department of Electrical and Electronics, Sri Venkateswara College of Engineering, Sriperumbudur, Chennai. He worked as a Design Engineer with the Electrical and Automotive Parts Manufacturing Unit, AA Industries, Chennai. He worked as a Visiting Scholar with the Clean and Resilient Energy Systems (CARES) Laboratory, Texas A&M University, Galveston, TX, USA. He currently works as a Subject Matter Expert with the Power and Energy (Research and Development Unit), Nestlives Pvt. Ltd., Chennai. He has published papers in international journals and international and national conferences. His research interest include PV cooling techniques, renewable energy and smart grids, wind energy research, power system operation and control, artificial intelligence, control techniques, and demand side management. He is a Department Topper and a Gold Medalist in his master's degree. He is also a recognized as a Reviewer in reputed journals, such as IEEE Systems Journal, IEEE Access, *IEEE Communications Magazine*, *International Transactions on Electrical Energy Systems* (Wiley), *Energy Sources Part A: Recovery, Utilization, and Environmental Effects* (Taylor and Francis), *Scientific Reports* (Springer Nature), *Chemical Engineering Journal* (Elsevier), *CFD Letters*, and *3 Biotech* (Springer).

SACHIN KUMAR (Senior Member, IEEE) was born in Dehradun, Uttarakhand, India. He received the B.Tech. degree in electrical engineering from Harcourt Butler Technological University (formerly Harcourt Butler Technological Institute), Kanpur, Uttar Pradesh, India, in 2008, the M.Tech. degree in power system engineering from the Indian Institute of Technology Kharagpur, West Bengal, India, in 2010. and the Ph.D. degree in electrical engineering from the Indian Institute of Technology (BHU), Varanasi, Uttar Pradesh, in 2021. He is currently working as an Assistant Professor with the Department of Electrical Engineering, Govind Ballabh Pant Institute of Engineering and Technology, Ghurdauri, Pauri-Garhwal, Uttarakhand, India. He has published more than 20 research articles in the indexed international journals and book chapters in prestigious handbooks. His research interests include reliability engineering, power system reliability, renewable energy systems, and green energy conversion systems. He is a Reviewer of IEEE Access, *IET Renewable Power Generation*, and *International Transactions on Electrical Energy Systems* (Wiley), and River Publishers, Denmark.

ANKIT KUMAR SRIVASTAVA received the B.Tech. degree in electrical engineering from the V. B. S. Purvanchal University, Jaunpur, Uttar Pradesh, India, the M.Tech. degree in power electronics and drives from the Kamla Nehru Institute of Technology, Sultanpur, Uttar Pradesh, India, and the Ph.D. degree from Dr. A.P.J. Abdul Kalam Technical University, Lucknow, Uttar Pradesh, India. He is currently working as an Assistant Professor with the Department of Electrical Engineering, Institute of Engineering and Technology, Dr. Rammanohar Lohia Avadh University, Ayodhya, India. He has published several papers in reputed international journals and various national/international conferences. His current interests include the area of short-term load and price forecasting, AI applications in power systems, computational Intelligence, and renewable energy.

BASEEM KHAN (Senior Member, IEEE) received the B.E. degree in electrical engineering from Rajiv Gandhi Technological University, in 2008, and the M.Tech. and Ph.D. degrees in electrical engineering from the Maulana Azad National Institute of Technology, India, in 2010 and 2014, respectively. He is currently working as a Faculty Member at Hawassa University, Ethiopia. He has published more than 125 research articles in indexed journals, including the IEEE Transactions, IEEE Access, *Computer and Electrical Engineering* (Elsevier), *IET GTD*, *IET RPG*, and *IET Power Electronics*. Further, he has authored and edited books with Wiley, CRC Press, and Elsevier. His research interests include power system restructuring, power system planning, smart grid, meta-heuristic optimization techniques, reliability analysis of renewable energy systems, power quality analysis, and renewable energy integration.